CAMTP

Center for Applied Mathematics and Theoretical Physics
University of Maribor • Maribor • Slovenia • EU

www.camtp.uni-mb.si

Introduction to Quantum Chaos

Marko Robnik

DYNAMICAL SYSTEMS AND COMPLEXITY

30th Summer School – Conference

Aristotle University Thessaloniki

Calandra, Halkidiki, 28 August - 6 September 2024

ABSTRACT

Chaos (chaotic behaviour) can emerge in deterministic systems of classical dynamics. It is due to the sensitive dependence on initial conditions, meaning that two nearby initial states of a system develop in time such that their positions (states) separate very fast (exponentially) in time. After a finite time (Lyapunov time) the accuracy of orbit characterizing the state of the system is entirely lost, the system could be in any allowed state. The system can be also ergodic, meaning that one single orbit describing the evolution of the system visits any other neighbourhood of all other states of the system. In this sense, chaotic behaviour in time evolution does not exist in quantum mechanics. However, if we look at the structural and statistical properties of the quantum system, we do find clear analogies and relationships with the structures of the corresponding classical systems. This is manifested in the eigenstates and energy spectra of various quantum systems (mesoscopic solid state systems, molecules, atoms, nuclei, elementary particles) and other wave systems (electromagnetic, acoustic, elastic, seismic, water surface waves etc), which are observed in nature and in the experiments. Here we review the basic aspects of quantum chaos in Hamiltonian systems. We shall focus on the most general (generic) systems, also called mixed-type systems, as their classical counterparts in the phase space exhibit regular regions coexisting with the chaotic regions for

complementary initial conditions. We shall review the basic concepts of quantum chaos in the stationary picture, that is the properties of the eigenstates of the stationary Schrödinger equation, the structure of wave functions, and of the corresponding Wigner functions in the quantum phase space, and the statistical properties of the energy spectra. Before treating the general mixed-type case we shall review the two extreme cases, the universality classes, namely the regular (integrable) systems, and the fully chaotic (ergodic) systems. Then the Berry-Robnik (1984) picture will be presented, and the underlying Principle of Uniform Semiclassical Condensation (PUSC) of the Wigner functions. Next, we shall consider the effects of quantum (dynamical) localization, which set in when the classical transport time (like diffusion time) is longer than the Heisenberg time scale (defined as the Planck constant divided by the mean energy level spacing). It will be shown phenomenologically that in the case of chaotic eigenstates in the quantum phase space (Wigner functions) the energy spectra display Brody level spacing distribution, where the level repulsion exponent (Brody parameter) goes from zero in the strongest localization to 1 in the fully extended states. The Berry-Robnik picture is then appropriately generalized to include the localization effects. Furthermore, the localization measures of chaotic localized eigenstates have a distribution, which in the absence of stickiness structures in the classical phase space is well described by the beta distribution. We neglect, at high energies, the tunneling effects coupling the regular and chaotic levels, since they are manifested only in low-lying levels, because the coupling decreases exponentially with increasing energy (or inverse effective Planck constant). Finally, we show that the relative fraction of mixed-type

eigenstates (classified by their Husimi functions) decreases in the semiclassical limit as a power law with the decreasing effective Planck constant (or equivalent semiclassical parameter), in agreement with and confirming PUCS.

Hamiltonian systems (1)

$$H = H(\vec{q}, \vec{p})$$

$$\vec{q} = (q_1, q_2, \dots, q_N)$$
$$\vec{p} = (p_1, p_2, \dots, p_N)$$

$$\begin{cases} \dot{\vec{q}} = \dfrac{\partial H}{\partial \vec{p}} \\ \dot{\vec{p}} = -\dfrac{\partial H}{\partial \vec{q}} \end{cases}$$

Hamilton equations

autonomous systems: $E = H(\vec{q}, \vec{p}) = \text{const.}$

$$H = \frac{\vec{p}^{\,2}}{2m} + V(\vec{q})$$

$$m\ddot{\vec{q}} = \dot{\vec{p}} = -\frac{\partial V}{\partial \vec{q}}$$

Newton eqs.

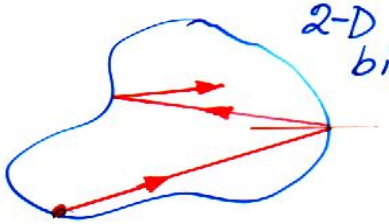

2-D billiards

$$\hat{H} = H(\hat{\vec{q}}, \hat{\vec{p}}), \quad \hat{\vec{q}} = \vec{q}, \quad \hat{\vec{p}} = \frac{\hbar}{i}\frac{\partial}{\partial \vec{q}}$$

$$\hat{H} = -\frac{\hbar^2}{2m}\Delta + V(\vec{q}), \quad \hat{H}\psi = E\psi$$

$$-\frac{\hbar^2}{2m}\Delta\psi + (V(\vec{q}) - E)\psi = 0$$

Schrödinger equation plus boundary conditions

billiards: $\Delta\psi + \dfrac{2m}{\hbar^2}E\psi = 0$

$$\psi|_{\partial B} \equiv 0$$

integrable Hamiltonian systems:

N integrals (constants) of motion exist

N = number of degrees of freedom

$A_i = A_i(\vec{q},\vec{p}) = A_i(\vec{q}(t),\vec{p}(t)) = \text{const.}$

$i = 1, 2, \ldots, N \qquad (A_1 = E = H(\vec{q},\vec{p}))$

$\{A_i, A_j\}$ = Poisson bracket $= 0, \forall i,j$

$$= \frac{\partial A_i}{\partial \vec{q}} \cdot \frac{\partial A_j}{\partial \vec{p}} - \frac{\partial A_i}{\partial \vec{p}} \cdot \frac{\partial A_j}{\partial \vec{q}} \equiv 0$$

Liouville-Arnold theorem:

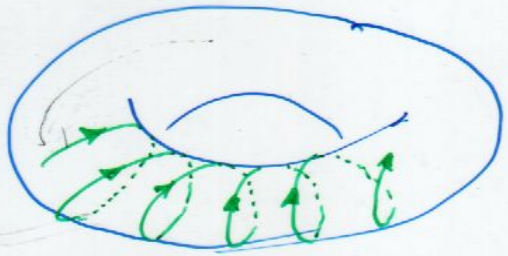

example ($N=2$)

N-dim invariant tori (for all initial conditions)

The ergodic systems (fully chaotic):

no integrals of motion except the total energy $E = H(\vec{q},\vec{p}) = \text{const.}$

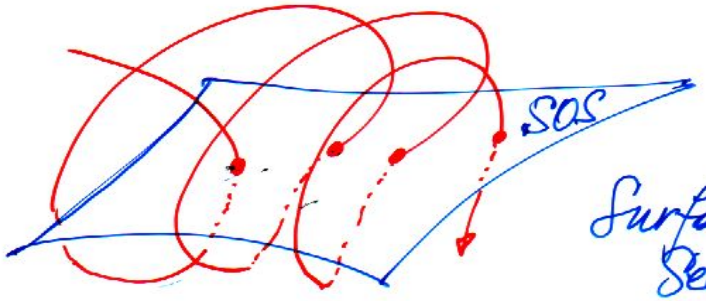

Surface of Section

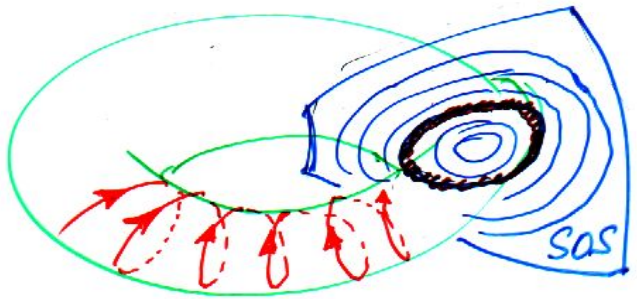

integrable: N-tori everywhere

perturb

Kolmogorov Arnold Moser

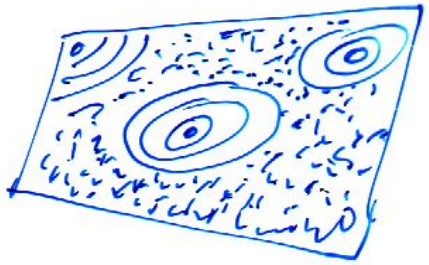

KAM picture

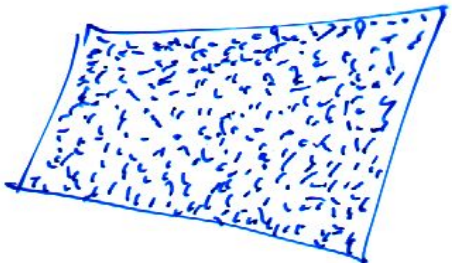

ergodic and chaotic

Example of mixed type system: Hydrogen atom in strong magnetic field

$$H = \frac{\mathbf{p}^2}{2m_e} - \frac{e^2}{r} + \frac{eL_z}{2m_e c}|\mathbf{B}| + \frac{e^2\mathbf{B}^2}{8m_e c^2}\rho^2$$

$\mathbf{B}$ = magnetic field strength vector pointing in z-direction

$r = \sqrt{x^2+y^2+z^2}$ = spherical radius, $\rho = \sqrt{x^2+y^2}$ = axial radius

L_z = z-component of angular momentum = conserved quantity

Characteristic field strength: $B_0 = \frac{m_e^2 e^3 c}{\hbar^2} = 2.35 \times 10^9$ Gauss $= 2.35 \times 10^5$ Tesla

Rough qualitative criterion for global chaos: magnetic force $\approx$ Coulomb force

(Wunner et al 1978+; Wintgen et al 1987+; Hasegawa, R. and Wunner 1989, Friedrich and Wintgen 1989; classical and quantum chaos: R. 1980+)

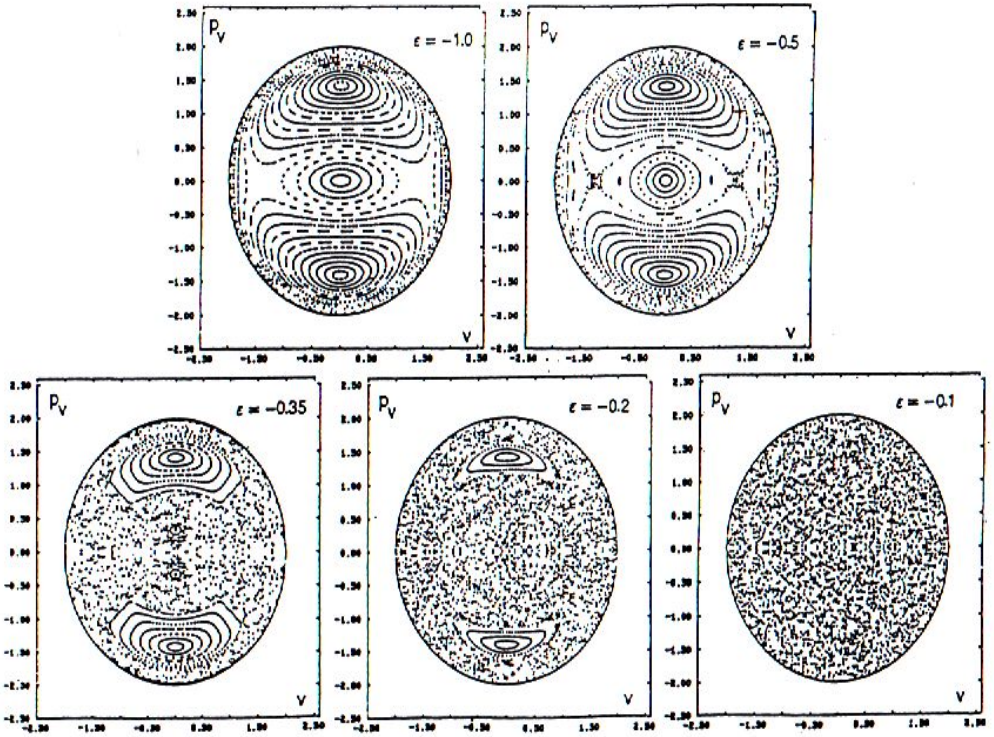

Fig. III-9. Poincaré surfaces of section $\Sigma(v, p_v; u=0)$ at different scaled energies (corresponding to increasing diamagnetic strength). The elliptic fixed point at the origin corresponds to the straight-line orbit I_∞, the other two fixed points to the straight-line orbit I_1.

Fig.I.8 - Segments of "spectra", each containing 50 levels. The "arrowheads" mark the occurrence of pairs of levels with spacings smaller than 1/4. See text for further explanation.

Bohigas and Giannoni 1984

Example: 2-dim billiard systems

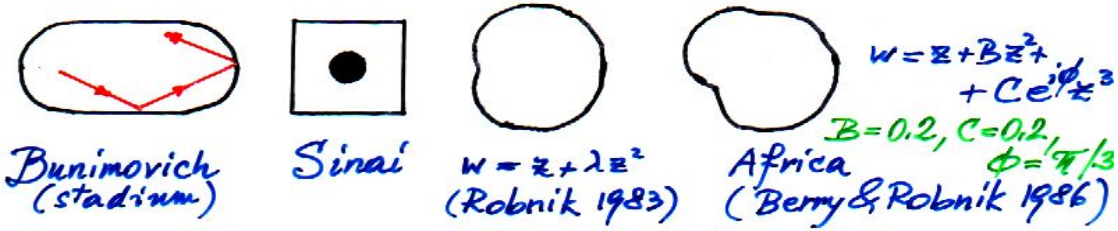

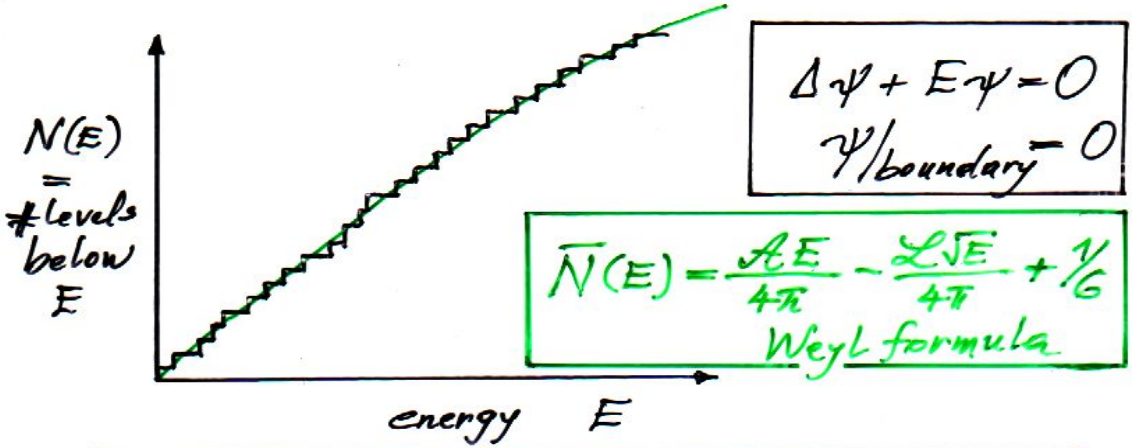

$$\Delta\psi + E\psi = 0$$
$$\psi/_{\text{boundary}} = 0$$

$$\bar{N}(E) = \frac{\mathcal{A}E}{4\pi} - \frac{\mathcal{L}\sqrt{E}}{4\pi} + \frac{\chi}{6}$$

Weyl formula

$$N(E) = \bar{N}(E) + \tilde{N}(E)$$

Unfolding procedure: $x \equiv \bar{N}(E) = x(E)$

$$N(x) = x + \tilde{N}(x)$$

- level spacings distribution: $P(S)$

  $P(S)\,dS$ = Prob. level spacing $S \in [S, S+dS]$

  normalized: $\int_0^\infty P(x)\,dx = 1$, $\int_0^\infty x\,P(x)\,dx = 1$

  cumulative: $W(S) = \int_0^S P(x)\,dx$

spectral unfolding procedure: transform the energy spectrum to unit mean level spacing (or density)

After such **spectral unfolding procedure** we are describing the spectral statistical properties, that is statistical properties of the eigenvalues.

Two are most important:

Level spacing distribution: P(S)

$P(S)dS =$ Probability that a nearest level spacing S is within $(S, S + dS)$

E(k,L) = probability of having precisely k levels on an interval of length L

Important special case is **the gap probability** $E(0, L) = E(L)$ of having no levels on an interval of length L, and is related to the level spacing distribution:

$$P(S) = \frac{d^2 E(S)}{dS^2}$$

The Gaussian Random Matrix Theory

$P(\{H_{ij}\})d\{H_{ij}\} =$ probability of the matrix elements $\{H_{ij}\}$ inside the volume element $d\{H_{ij}\}$

We are looking for the statistical properties of the eigenvalues

A1 $P(\{H_{ij}\}) = P(\mathbf{H})$ is invariant against the group transformations, which preserve the structure of the matrix ensemble:

orthogonal transformations for the real symmetric matrices: **GOE**
unitary transformations for the complex Hermitian matrices: **GUE**

It follows that $P(\mathbf{H})$ must be a function of the invariants of $\mathbf{H}$

A2 The matrix elements are statistically independently distributed:

$$P(H_{11}, \ldots, H_{NN}) = P(H_{11}) \ldots P(H_{NN})$$

It follows from these two assumptions that the distribution $P(H_{ij})$ must be Gaussian:

There is no free parameter: Universality

2D GOE and GUE of random matrices:

Quite generally, for a Hermitian matrix $\begin{pmatrix} x & y+iz \\ y-iz & -x \end{pmatrix}$ with x, y, z real

the eigenvalue $\lambda = \pm\sqrt{x^2+y^2+z^2}$ and level spacing
$S = \lambda_1 - \lambda_2 = 2\sqrt{x^2+y^2+z^2}$

The level spacing distribution is

$$P(S) = \int_{R^3} dx\, dy\, dz\, g_x(x) g_y(y) g_z(z) \delta(S - 2\sqrt{x^2+y^2+z^2}) \qquad (1)$$

which is equivalent to 2D GOE/GUE when $g_x(u) = g_y(u) = g_z(u) = \frac{1}{\sigma\sqrt{\pi}} \exp(-\frac{u^2}{\sigma^2})$
and after normalization to $< S >= 1$

- **2D GUE** $P(S) = \frac{32S^2}{\pi^2} \exp(-\frac{4S^2}{\pi})$ Quadratic level repulsion

- **2D GOE** $g_z(u) = \delta(u)$ and $P(S) = \frac{\pi S}{2} \exp(-\frac{\pi S^2}{4})$ Linear level repulsion

There is no free parameter: Universality

ENERGY (NEAREST NEIGHBOUR)
LEVEL SPACING DISTRIBUTION
$P(S)$

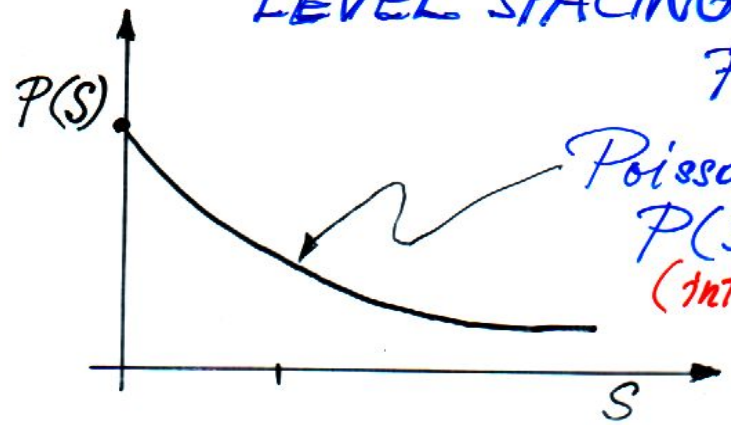

Poisson
$P(S) = e^{-S}$
(integrability)

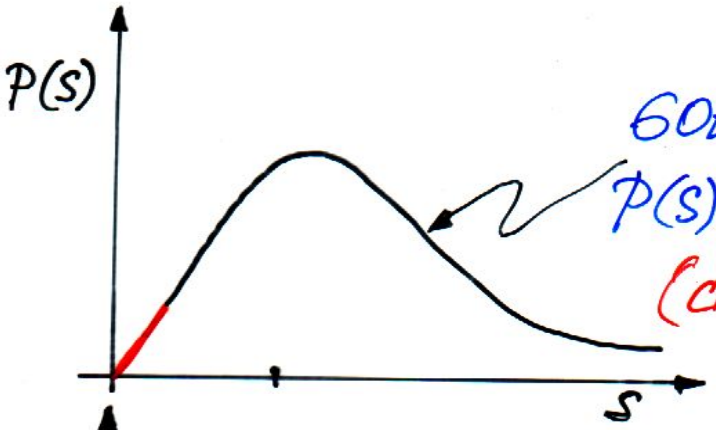

GOE ≈ Wigner
$P(S) = \frac{\pi S}{2} e^{-\frac{\pi S^2}{4}}$
(chaos & A.U.S.)

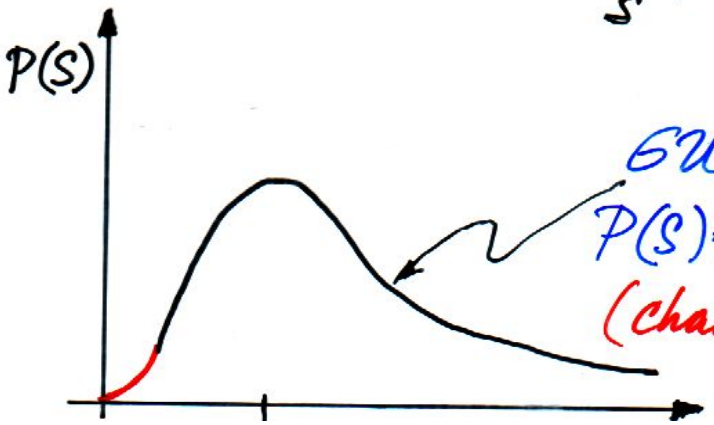

GUE ≈ Wigner
$P(S) = \frac{32 S^2}{\pi^2} e^{-\frac{4S^2}{\pi}}$
(chaos, no A.U.S.)

The Main Assertion of Stationary Quantum Chaos
(Casati, Valz-Gries, Guarneri 1980; Bohigas, Giannoni, Schmit 1984; Percival 1973)

(A1) If the system is classically integrable: **Poissonian spectral statistics**

(A2) If classically fully chaotic (ergodic): **Random Matrix Theory (RMT)** applies

- If there is an antiunitary symmetry, we have GOE statistics
- If there is no antiunitary symmetry, we have GUE statistics

(A3) If of the mixed type, in the deep semiclassical limit: we have no spectral correlations: the spectrum is a **statistically independent superposition of regular and chaotic level sequences**:

$$E(k,L) = \sum_{k_1+k_2+\ldots+k_m=k} \prod_{j=1}^{j=m} E_j(k_j, \mu_j L) \qquad (2)$$

μ_j= relative fraction of phase space volume = relative density of corresponding quantum levels. $j=1$ is the Poissonian, $j \geq 2$ chaotic, and $\mu_1 + \mu_2 + \ldots + \mu_m = 1$

According to our theory, for a two-component system, $j = 1, 2$, we have (Berry and Robnik 1984):

$$E(0, S) = E_1(0, \mu_1 S) E_2(0, \mu_2 S)$$

Poisson (regular) component: $E_1(0, S) = e^{-S}$

Chaotic (irregular) component: $E_2(0, S) = \mathrm{erfc}\left(\frac{\sqrt{\pi} S}{2}\right)$ (Wigner = 2D GOE)

$E(0, S) = E_1(0, \mu_1 S) E_2(0, \mu_2 S) = e^{-\mu_1 S} \mathrm{erfc}(\frac{\sqrt{\pi} \mu_2 S}{2})$, where $\mu_1 + \mu_2 = 1$.

Then $P(S) =$ level spacing distribution $= \frac{d^2 E(0,S)}{dS^2}$ and we obtain:

$P_{BR}(S) = e^{-\mu_1 S} \left(\exp(-\frac{\pi \mu_2^2 S^2}{4}) (2\mu_1 \mu_2 + \frac{\pi \mu_2^3 S}{2}) + \mu_1^2 \mathrm{erfc}(\frac{\mu_2 \sqrt{\pi} S}{2}) \right)$
(Berry and Robnik 1984)

This is a one parameter family of distribution functions with normalized total probability $< 1 >= 1$ and mean level spacing $< S >= 1$, whilst the second moment can be expressed in the closed form and is a function of μ_1.

2. Recent results on the energy level statistics in the transition region between integrability and chaos

fractional volume:
regular regions ρ_1
chaotic region ρ_2

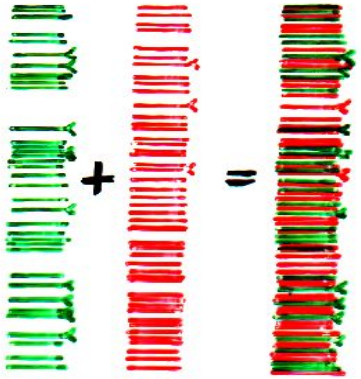

Berry & Robnik 1984
(statistical independence)

Poisson $\langle \Delta E \rangle = 1/\rho_1$ GOE $\langle \Delta E \rangle = 1/\rho_2$ $\langle \Delta E \rangle = 1$ $(\rho_1 + \rho_2 = 1)$

$$P_1(S) = \rho_1 e^{-\rho_1 S}, \quad P_j(S) \simeq \frac{\pi \rho_j^2 S}{2} \exp\left(-\frac{\pi}{4}\rho_j^2 S^2\right)$$

The answer:

$$P(S) = \frac{d^2 Z}{dS^2}, \quad Z(S) = \prod_{j=1}^{m} \rho_j Z_j(S)$$

where $Z_j(S) = \int_S^\infty dt\, P_j(t)(t-S)$

$$P_m(S) = \frac{d^2}{dS^2}\left[e^{-\rho_1 S} \prod_{j=2}^{m} \operatorname{erfc}\left(\frac{\sqrt{\pi}}{2}\rho_j S\right)\right]$$

$$\operatorname{erfc}(x) \equiv \frac{2}{\sqrt{\pi}} \int_x^\infty dt\, e^{-t^2}$$

and (as a consequence of the statistical independence)

$$P_m(S=0) = 1 - \sum_{j=2}^{m} \varrho_j^2$$

Special case $m=2$:

$$P_2(S,\varrho_1) = \varrho_1^2 e^{\varrho_1 S} \operatorname{erfc}\left(\frac{\sqrt{\pi}}{2}\varrho_2 S\right) + (2\varrho_1\varrho_2 + \tfrac{1}{2}\pi\varrho_2^3 S)\exp\left(-\varrho_1 S - \tfrac{1}{4}\pi\varrho_2^2 S^2\right)$$

and

$$P_2(S=0,\varrho_1) = 1-\varrho_2^2 = \varrho_1(2-\varrho_1)$$

vanishes only if $\varrho_1=0$, $\varrho_2=1$

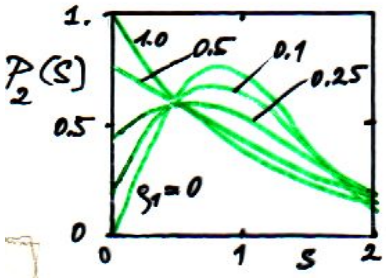

Berry & Robnik 1984

Similarly, upon the assumption of statistical independence:

$$\Delta(L) = \sum_{j=1}^{m} \Delta_j(\varrho_j L)$$

(Seligman and Verbaarschot 1985)

$W = z + \lambda z^2$ (Robnik 1983) $\lambda = 0.15$

Figure 1

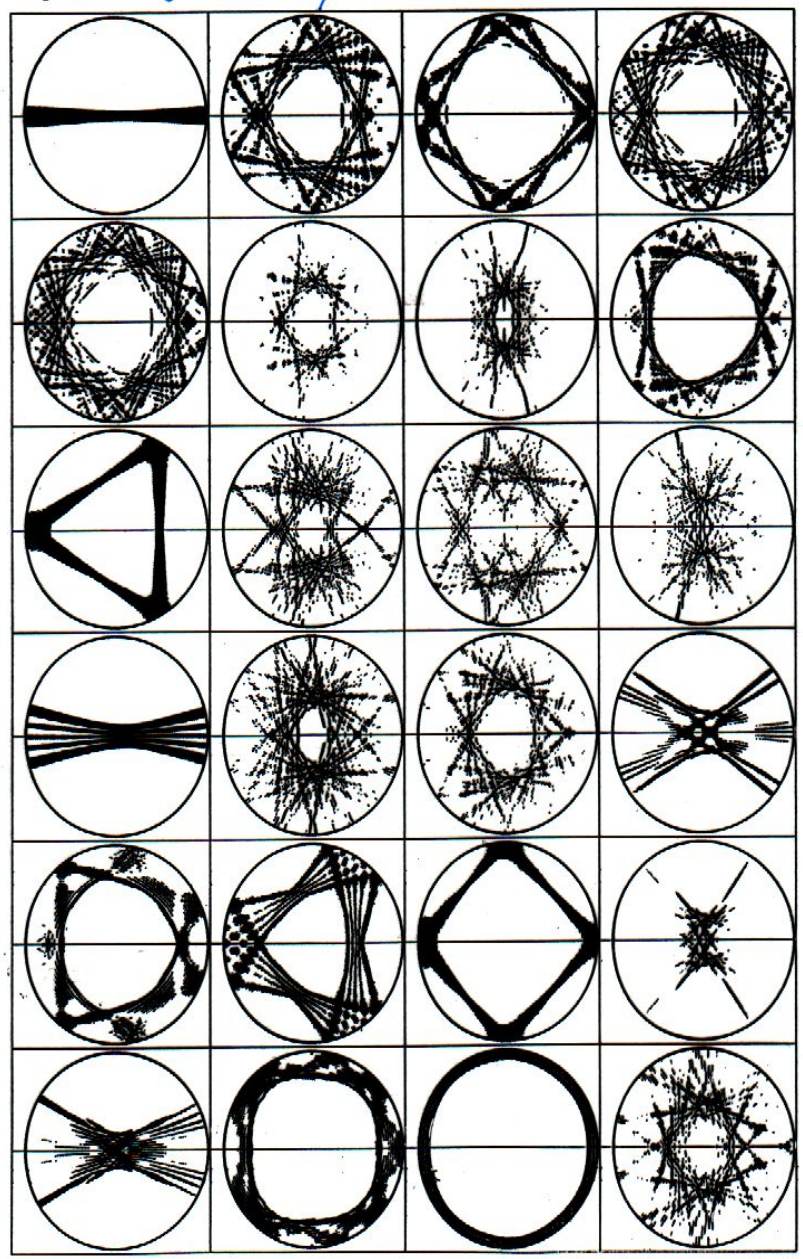

2. Principle of Uniform Semiclassical Condensation (PUSC) of Wigner functions of eigenstates (Percival 1973, Berry 1977, Shnirelman 1979, Voros 1979, Robnik 1987-1998)

We study the structure of eigenstates in "quantum phase space": **The Wigner functions of eigenstates** (they are real valued but **not positive definite**):

Definition: $W_n(\mathbf{q},\mathbf{p}) = \frac{1}{(2\pi\hbar)^N}\int d^N\mathbf{X}\exp\left(-\frac{i}{\hbar}\mathbf{p}.\mathbf{X}\right)\psi_n(\mathbf{q}-\frac{\mathbf{X}}{2})\psi_n^*(\mathbf{q}+\frac{\mathbf{X}}{2})$

$(P1)\quad \int W_n(\mathbf{q},\mathbf{p})d^N\mathbf{p} = |\psi_n(\mathbf{q})|^2$

$(P2)\quad \int W_n(\mathbf{q},\mathbf{p})d^N\mathbf{q} = |\phi_n(\mathbf{p})|^2$

$(P3)\quad \int W_n(\mathbf{q},\mathbf{p})d^N\mathbf{q}\, d^N\mathbf{p} = 1$

$(P4)\quad (2\pi\hbar)^N\int d^N\mathbf{q}\, d^N\mathbf{p} W_n(\mathbf{q},\mathbf{p})W_m(\mathbf{q},\mathbf{p}) = \delta_{nm}$

$(P5)\quad |W_n(\mathbf{q},\mathbf{p})| \le \frac{1}{(\pi\hbar)^N}$ (Cauchy-Schwarz inequality)

$(P6 = P4)\quad \int W_n^2(\mathbf{q},\mathbf{p})d^N\mathbf{q}\, d^N\mathbf{p} = \frac{1}{(2\pi\hbar)^N}$

$(P7)\quad \hbar\to 0: \quad W_n(\mathbf{q},\mathbf{p}) \to (2\pi\hbar)^N W_n^2(\mathbf{q},\mathbf{p}) > 0$

In the semiclassical limit the Wigner functions condense on an element of phase space of volume size $(2\pi\hbar)^N$ (elementary quantum Planck cell) and become positive definite there.

Principle of Uniform Semiclassical Condensation (PUSC)

Wigner fun. $W_n(\mathbf{q},\mathbf{p})$ condenses uniformly on a classically invariant component:

(C1) invariant N-torus (integrable or KAM): $W_n(\mathbf{q},\mathbf{p}) = \frac{1}{(2\pi)^N}\delta\left(\mathbf{I}(\mathbf{q},\mathbf{p}) - \mathbf{I_n}\right)$

(C2) uniform on topologically transitive chaotic region:

$W_n(\mathbf{q},\mathbf{p}) = \frac{\delta(E_n - H(\mathbf{q},\mathbf{p}))\ \chi_\omega(\mathbf{q},\mathbf{p})}{\int d^N\mathbf{q}\ d^N\mathbf{p}\ \delta(E_n - H(\mathbf{q},\mathbf{p}))\ \chi_\omega(\mathbf{q},\mathbf{p})}$

where $\chi_\omega(\mathbf{q},\mathbf{p})$ is the characteristic function on the chaotic component indexed by ω

(C3) ergodicity: microcanonical: $W_n(\mathbf{q},\mathbf{p}) = \frac{\delta(E_n - H(\mathbf{q},\mathbf{p}))}{\int d^N\mathbf{q}\ d^N\mathbf{p}\ \delta(E_n - H(\mathbf{q},\mathbf{p})}$

Important: Relative Liouville measure of the classical invariant component:

$\mu(\omega) = \frac{\int d^N\mathbf{q}\ d^N\mathbf{p}\ \delta(E_n - H(\mathbf{q},\mathbf{p}))\ \chi_\omega(\mathbf{q},\mathbf{p})}{\int d^N\mathbf{q}\ d^N\mathbf{p}\ \delta(E_n - H(\mathbf{q},\mathbf{p}))}$

How good is this theory at sufficiently small effective $\hbar$?

Prosen and Robnik 1999

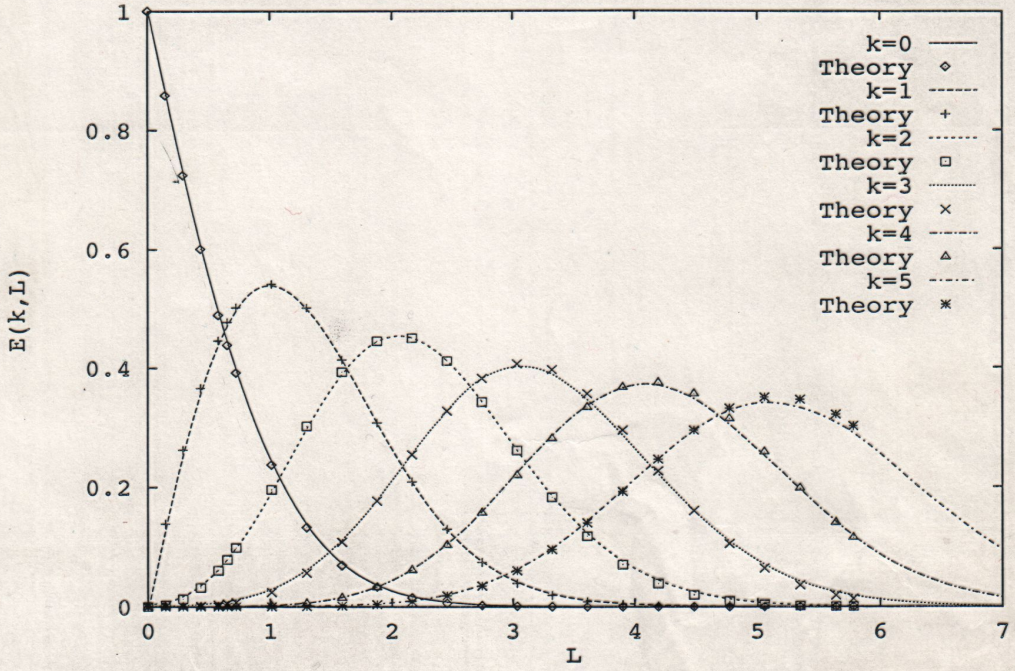

Figure 8: Same as in figure 1 but for 5168 consecutive levels of the quartic billiard (Prosen 1998) for $a = 0.04$ with sequential quantum number $\mathcal{N} \approx 8\,000\,000$, and for theoretical distributions with $\rho_1 = 0.12$.

quartic billiard $a = 0.04$

$r = 1 + a\cos(4\phi)$

4. Approach to describe the semiclassical transition regime

If we are not sufficiently deep in the semiclassical regime of sufficiently small effective Planck constant $\hbar_{eff}$, which e.g. in billiards means not at sufficiently high energies, we observe **two new effects**, which are the cause for the deviation from BR statistics:

• **Localization** of eigenstates, due to the **dynamical localization**: The Wigner functions are no longer uniformly spread over the classically available chaotic component but are localized instead.

• **Coupling** due to **tunneling** between the semiclassical regular (R) and chaotic (C) states

This effect typically disappears very quickly with increasing energy, due to the exponential dependence on $1/\hbar_{eff}$.

THE IMPORTANT SEMICLASSICAL CONDITION

The semiclassical condition for the random matrix theory to apply in the chaotic eigenstates is that the Heisenberg time t_H is larger than all classical transport times t_T of the system!

The Heisenberg time of any quantum system= $t_H = \frac{2\pi\hbar}{\Delta E} = 2\pi\hbar\rho(E)$

$\Delta E = 1/\rho(E)$ is the mean energy level spacing, $\rho(E)$ is the mean level density

The quantum evolution follows the classical evolution including the chaotic diffusion up to the Heisenberg time, at longer times the destructive interference sets in and causes:

the quantum or **dynamical localization** if $t_H \ll t_T$

Note: $\rho(E) \propto \frac{1}{(2\pi\hbar)^N} \to \infty$ when $\hbar \to 0$, and therefore eventually $t_H \gg t_T$.

This observation applies to time-dependent and to time-independent systems.

We shall illustrate the results in real billiard spectra.

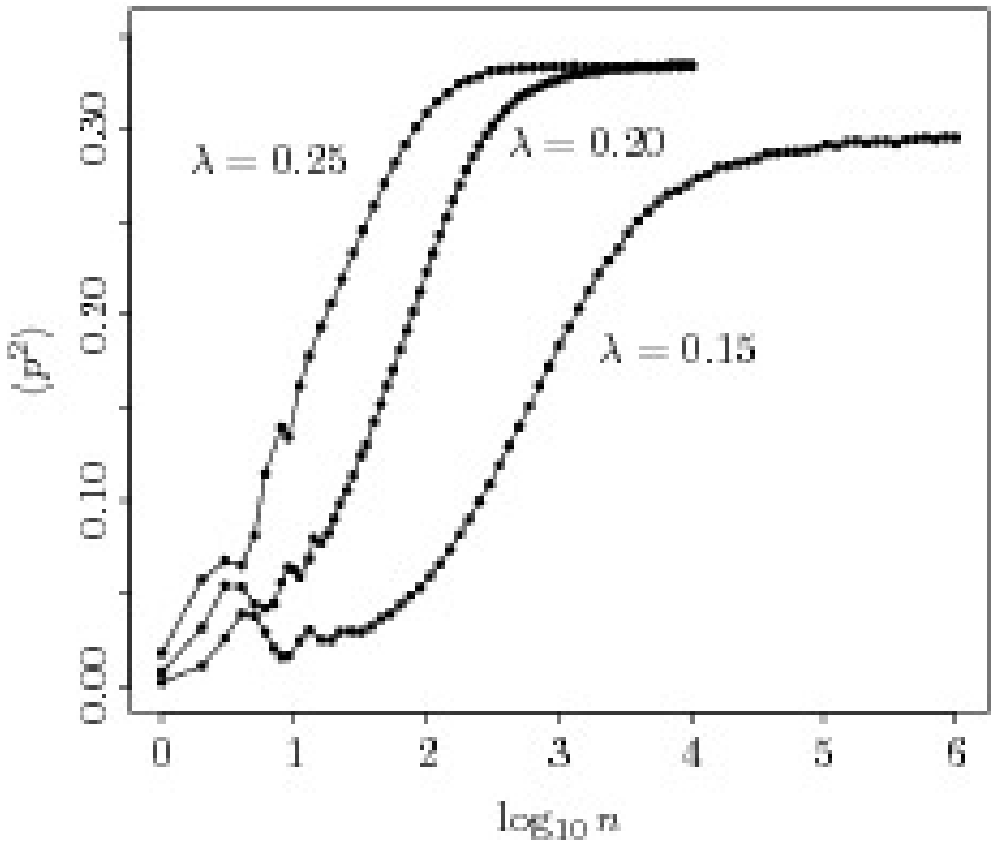

We show the second moment $\langle p^2 \rangle$ averaged over an ensemble of 10^6 initial conditions uniformly distributed in the chaotic component on the interval $s \in [0, \mathcal{L}/2]$ and $p = 0$.. We see that the saturation value of $\langle p^2 \rangle$ is reached at about $N_T = 10^5$ collisions for $\lambda = 0.15$, $N_T = 10^3$ collisions for $\lambda = 0.20$ and $N_T = 10^2$ for $\lambda = 0.25$. For $\lambda = 0.15$, according to the criterion at $k = 2000$ and $k = 4000$, we are still in the regime where the dynamical localization is expected. On the other hand, for $\lambda = 0.20, 0.25$ we expect extended states already at $k < 2000$.

Dynamically localized chaotic states are semiempirically well described by the Brody level spacing distribution: (Izrailev 1988,1989, Prosen and Robnik1993/4)

$$P_B(S) = C_1 S^\beta \exp\left(-C_2 S^{\beta+1}\right), \quad F_B(S) = 1 - W_B(S) = \exp\left(-C_2 S^{\beta+1}\right),$$

where $\beta \in [0,1]$ and the two parameters C_1 and C_2 are determined by the two normalizations $< 1 >=< S >= 1$, and are given by

$C_1 = (\beta+1)C_2, \quad C_2 = \left(\Gamma\left(\frac{\beta+2}{\beta+1}\right)\right)^{\beta+1}$ with $\Gamma(x)$ being the Gamma function. If we have extended chaotic states $\beta = 1$ and RMT applies, whilst in the strongly localized regime $\beta = 0$ and we have Poissonian statistics. The corresponding gap probability is

$$E_B(S) = \frac{1}{\Gamma\left(\frac{1}{\beta+1}\right)} Q\left(\frac{1}{\beta+1}, \left(\Gamma\left(\frac{\beta+2}{\beta+1}\right) S\right)^{\beta+1}\right)$$

$Q(\alpha, x)$ is the incomplete Gamma function: $Q(\alpha, x) = \int_x^\infty t^{\alpha-1} e^{-t} dt$.

The BRB theory: BR-Brody
(Prosen and Robnik 1993/1994, Batistić and Robnik 2010)

We have divided phase space $\mu_1 + \mu_2 = 1$ and localization β:

$$E(S) = E_r(\mu_1 S) E_c(\mu_2 S) = \exp(-\mu_1 S) E_{Brody}(\mu_2 S)$$

and the level spacing distribution $P(S)$ is:

$$P(S) = \frac{d^2 E_r}{dS^2} E_c + 2 \frac{dE_r}{dS} \frac{dE_c}{dS} + E_r \frac{d^2 E_c}{dS^2}$$

We study the billiard defined by the quadratic complex conformal mapping: $w(z) = z + \lambda z^2$ of the unit circle $|z| = 1$ (introduced in R. 1983/1984).

We choose $\lambda = 0.15$, for which $\rho_1 = 0.175$

We plot the level spacing distribution $P(S)$

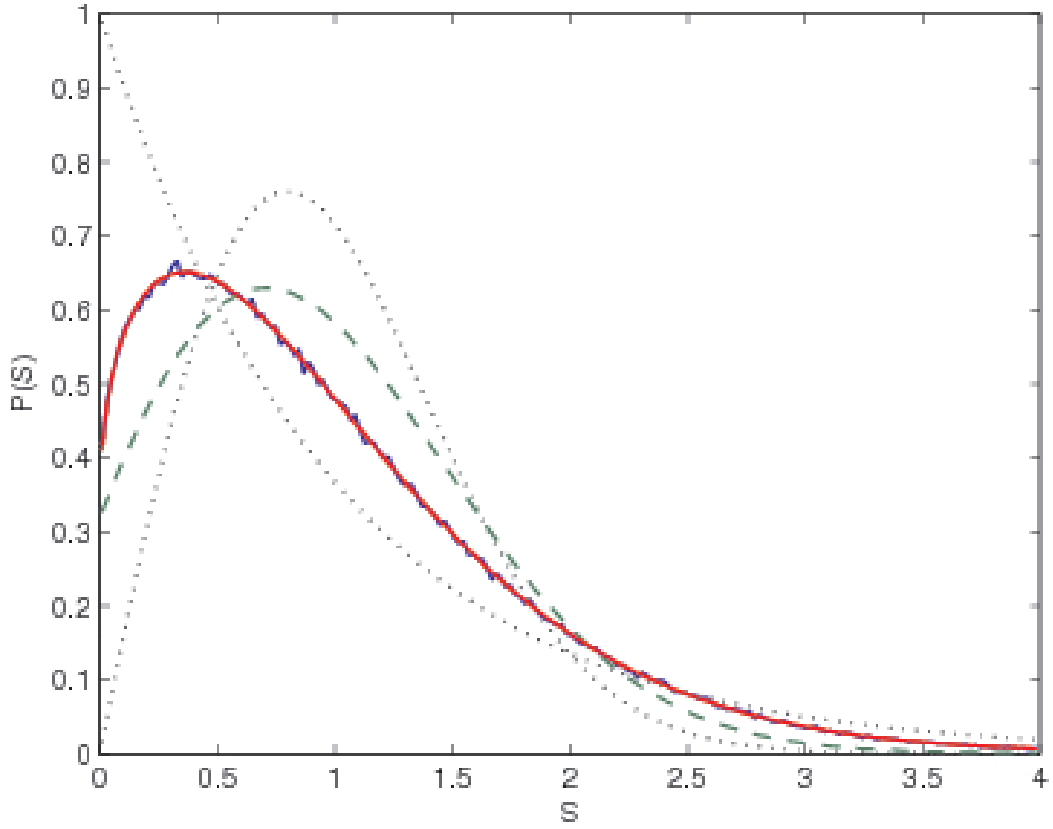

The level spacing distribution for the billiard $\lambda = 0.15$, compared with the analytical formula for BRB (red full line) with parameter values $\rho_1 = 0.183$, $\beta = 0.465$ and $\sigma = 0$. The dashed red curve close to the full red line is BRB with classical $\rho_1 = 0.175$ is not visible, as it overlaps completely with the quantum case $\rho_1 = 0.183$. The dashed curve far away from the red full line is just the BR curve with the classical $\rho_1 = 0.175$. The Poisson and GOE curves (dotted) are shown for comparison. The agreement of the numerical spectra with BRB is perfect. In the histogram we have 650000 objects, and the statistical significance is extremely large.

Separating the regular and chaotic eigenstates in a mixed-type billiard system
recent work by Batistić and Robnik 2013

The idea:

Introduce the quantum phase space analogous to the classical billiard phase space in Poincaré-Birkhoff coordinates, by using the Husimi functions in the same space.

Look at the overlap of the quantum eigenstates with the classical regular and classically chaotic component(s), and thus separate the regular and chaotic eigenstates and also the corresponding energy eigenvalues.

Then perform the spectral statistical analysis separately for the regular and chaotic level sequences.

We find: Poisson for regular and Brody for chaotic eigenstates.

$$\Delta\psi + k^2\psi = 0, \quad \psi|_{\partial\mathcal{B}} = 0. \tag{3}$$

$$u(s) = \mathbf{n} \cdot \nabla_{\mathbf{r}} \psi \left(\mathbf{r}(s) \right), \tag{4}$$

$$u(s) = -2 \oint dt \; u(t) \; \mathbf{n} \cdot \nabla_{\mathbf{r}} G(\mathbf{r}, \mathbf{r}(t)). \tag{5}$$

$$G(\mathbf{r}, \mathbf{r}') = -\frac{i}{4} H_0^{(1)}(k|\mathbf{r} - \mathbf{r}'|), \tag{6}$$

$$\psi_j(\mathbf{r}) = - \oint dt \; u_j(t) \; G \left(\mathbf{r}, \mathbf{r}(t) \right). \tag{7}$$

$$c_{(q,p),k}(s) = \sum_{m \in \mathbf{Z}} \exp\{i \, k \, p \, (s - q + m\mathcal{L})\} \exp\left(-\frac{k}{2} (s - q + m\mathcal{L})^2 \right). \tag{8}$$

$$H_j(q,p) = \left| \int_{\partial\mathcal{B}} c_{(q,p),k_j}(s) \; u_j(s) \; ds \right|^2, \quad M = \sum_{i,j} H_{i,j} \; A_{i,j}. \tag{9}$$

Phase space overlap index: $M = \sum_{i,j} H_{i,j}\, A_{i,j}$

$H_{i,j}$ is the **Husimi function** at point (i,j): **normalized**: $\sum_{i,j} H_{i,j} = 1$.

$A_{i,j}$ is discrete characteristic function: -1 for regular, $+1$ for chaotic point (i,j)

Therefore:

$M = +1$ if all nonzero $H_{i,j}$ are in the chaotic region

$M = -1$ if all nonzero $H_{i,j}$ are in the regular region

In the strict semiclassical limit (PUSC) we have either $M = +1$, or $M = -1$.

However, at lower energies, larger effective Planck constant, $H_{i,j}$ can be partially in regular and chaotic region due to various mechanisms: $-1 < M < 1$.

Consequently, M has a **doubly peaked distribution at** ± 1, but such that **the fraction of intermediate values of** M **decays to zero as a power law** with decreasing Planck constant (increasing energy) in the semiclassical limit.

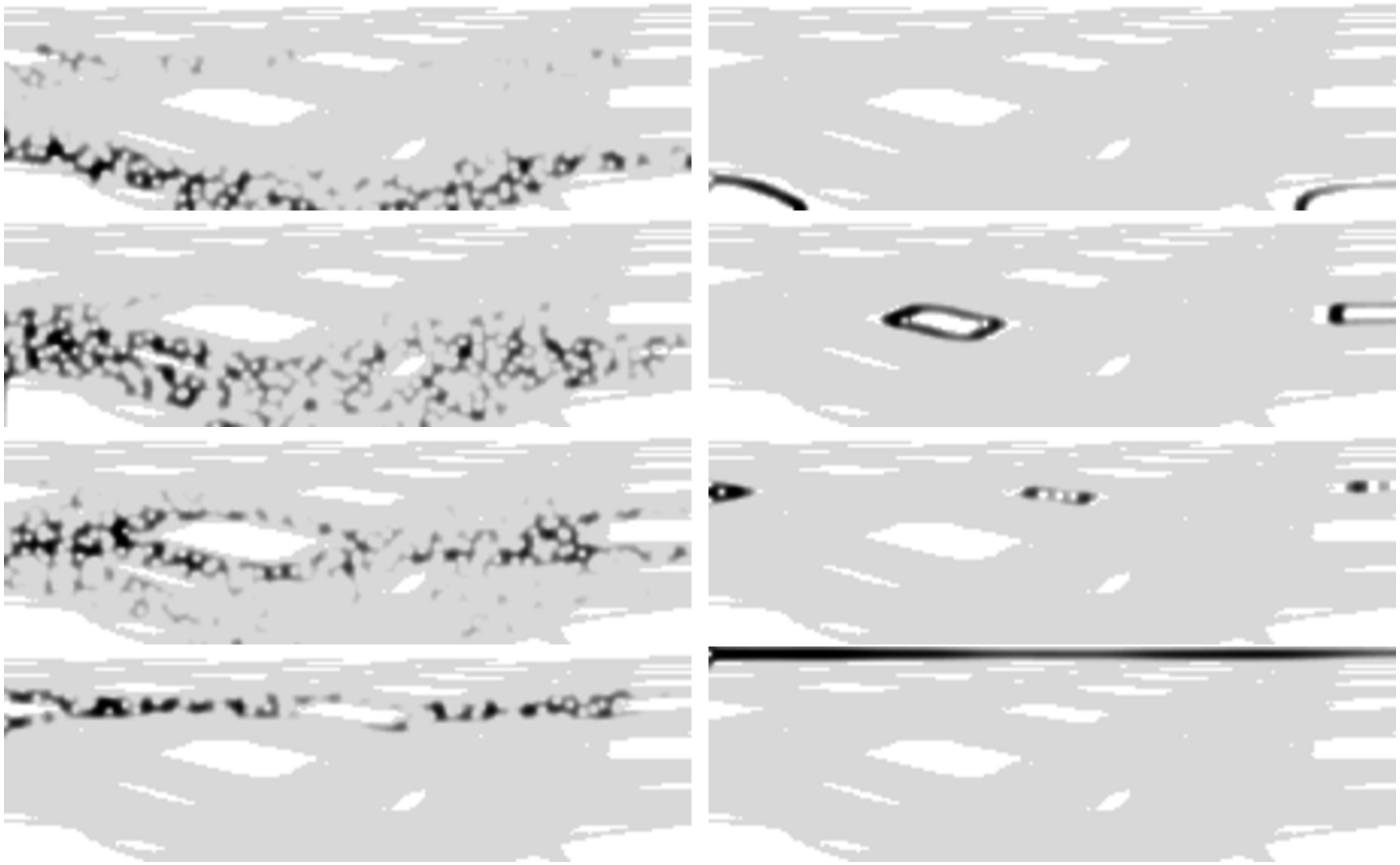

Examples of chaotic (left) and regular (right) states in the Poincaré-Husimi representation. $k_j\ (M)$ from top down are: chaotic: $k_j\ (M) =$ 2000.0021815 (0.978), 2000.0181794 (0.981), 2000.0000068 (0.989), 2000.0258600 (0.965); regular: $k_j\ (M) =$ 2000.0081402 (-0.987), 2000.0777155 (-0.821), 2000.0786759 (-0.528), 2000.0112417 (-0.829). The gray background is the classically chaotic invariant component. We show only one quarter of the surface of section $(s, p) \in [0, \mathcal{L}/2] \times [0, 1]$, because due to the reflection symmetry and time-reversal symmetry the four quadrants are equivalent.

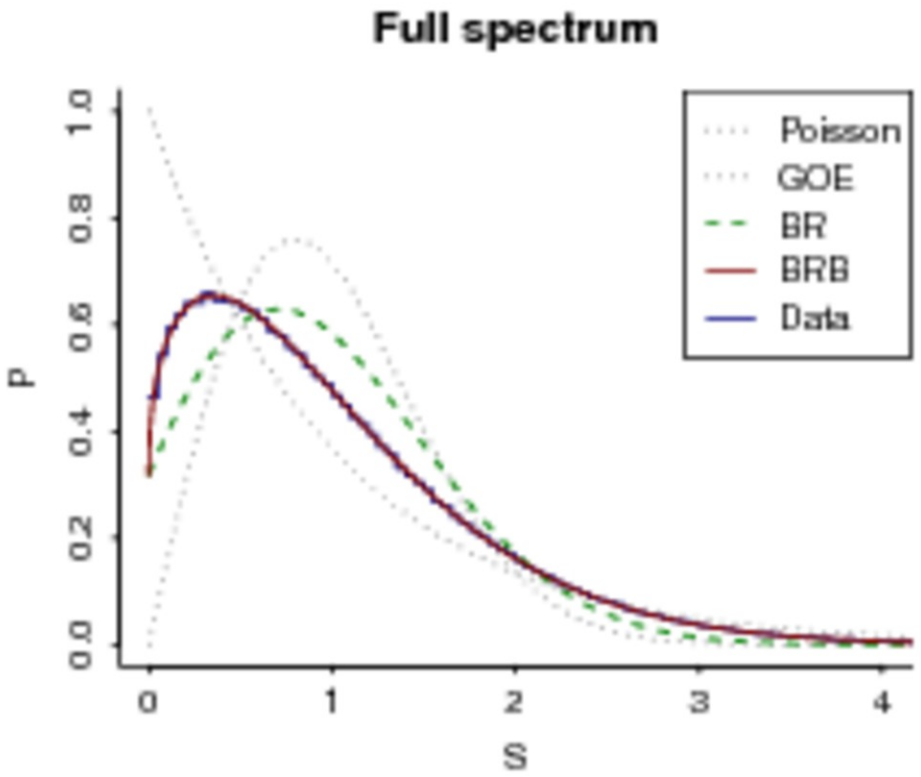

The level spacing distribution for the entire spectrum after unfolding for $N = 587653$ spacings, with $k_j \in [2000, 2500]$, in excellent agreement with the BRB distribution with the classical $\rho_1 = 0.175$ and $\beta = 0.45$.

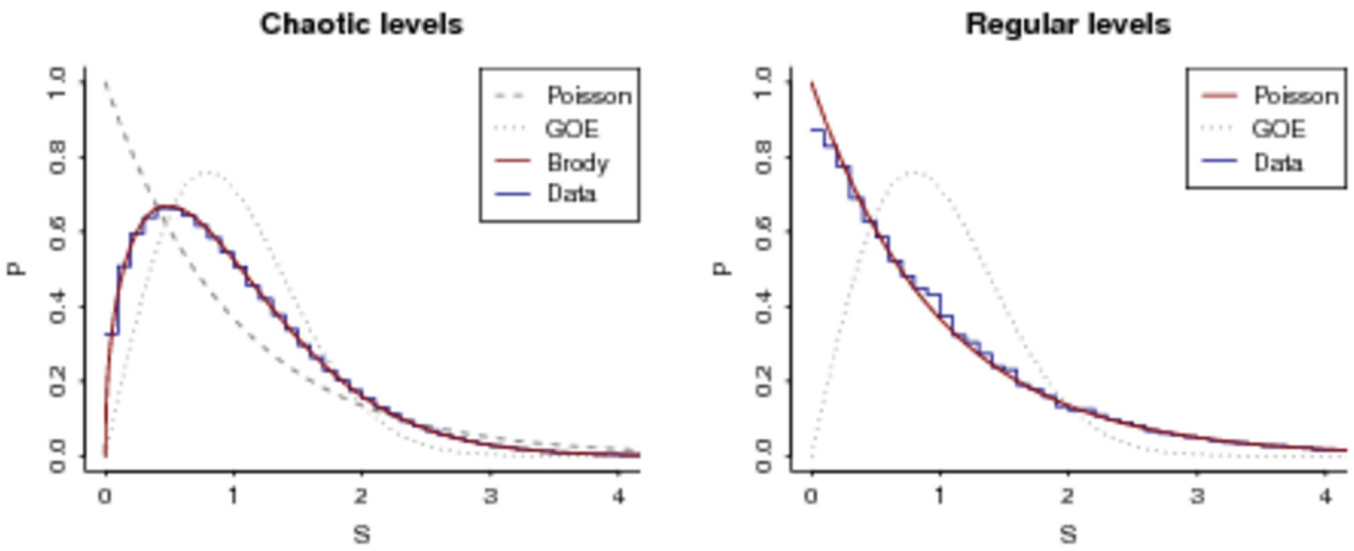

Separation of levels using the classical criterion $M_t = 0.431$. (a; left) The level spacing distribution for the chaotic subspectrum after unfolding, in perfect agreement with the Brody distribution $\beta = 0.444$. (b; right) The level spacing distribution for the regular part of the spectrum, after unfolding, in excellent agreement with Poisson.

The localization measures of chaotic eigenstates:
recent work by Batistić and Robnik 2013

A: localization measure based on **the information entropy** of the Husimi quasi-probability distribution:

Calculate normalized Husimi distribution $H(q,p)$ on the phase space (q,p) and then the information entropy for each chaotic eigenstate

$$I = -\int dq\, dp\, H(q,p) \ln\left((2\pi\hbar)^N H(q,p)\right)$$

and **define:** $A = \frac{\exp\langle I\rangle}{\Omega_C/(2\pi\hbar)^N}$ **(= entropy localization measure)**

where $\Omega_C =$ phase space volume on which $H(q,p)$ is defined, and the averaging is over a large number of consecutive chaotic eigenstates.

- Uniform distribution $H = 1/\Omega_C$: $A = 1$ (extendedness)
- Strongest localization in a single Planck cell: $H = 1/(2\pi\hbar)^N$

$$I = \ln\left((2\pi\hbar)^N H\right) = 0 \text{ and } A = (2\pi\hbar)^N/\Omega_C = 1/N_{Ch}(E) \approx 0$$

C: localization measure based on **the correlations** of the Husimi quasi-probability distribution:

Calculate normalized Husimi distribution $H_m(q,p)$ for each chaotic eigenstate labeled by m, and then the correlation matrix for large number of consecutive chaotic eigenstates:

$$C_{nm} = \frac{1}{Q_n Q_m} \int dq\, dp\, H_n(q,p)\, H_m(q,p)$$

where $Q_n = \sqrt{\int dq\, dp\, H_n^2(q,p)}$ is the normalizing factor

and define

$$C = \langle C_{nm} \rangle \quad \textbf{(= correlation localization measure)}$$

where the averaging is over a large number of consecutive chaotic eigenstates

Surprisingly and satisfactory: The two localization measures A and C are linearly related and thus equivalent !

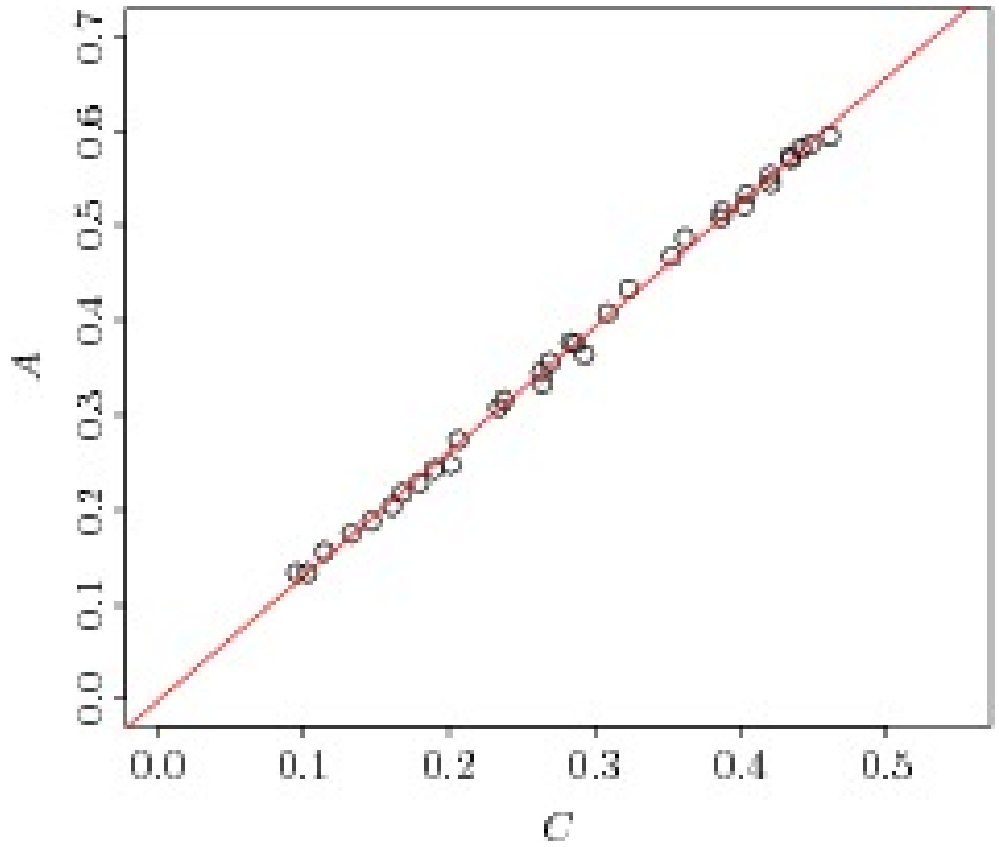

Linear relation between the two entirely different localization measures, namely the entropy measure A and the correlation measure C, calculated for several different billiards at $k \approx 2000$ and $k \approx 4000$.

As expected and in analogy to time-periodic systems like quantum kicked rotator: The spectral Brody parameter β, describing the level repulsion in the level spacing distribution $P(S) \propto S^{\beta}$ at small S is functionally related to the localization measure A:

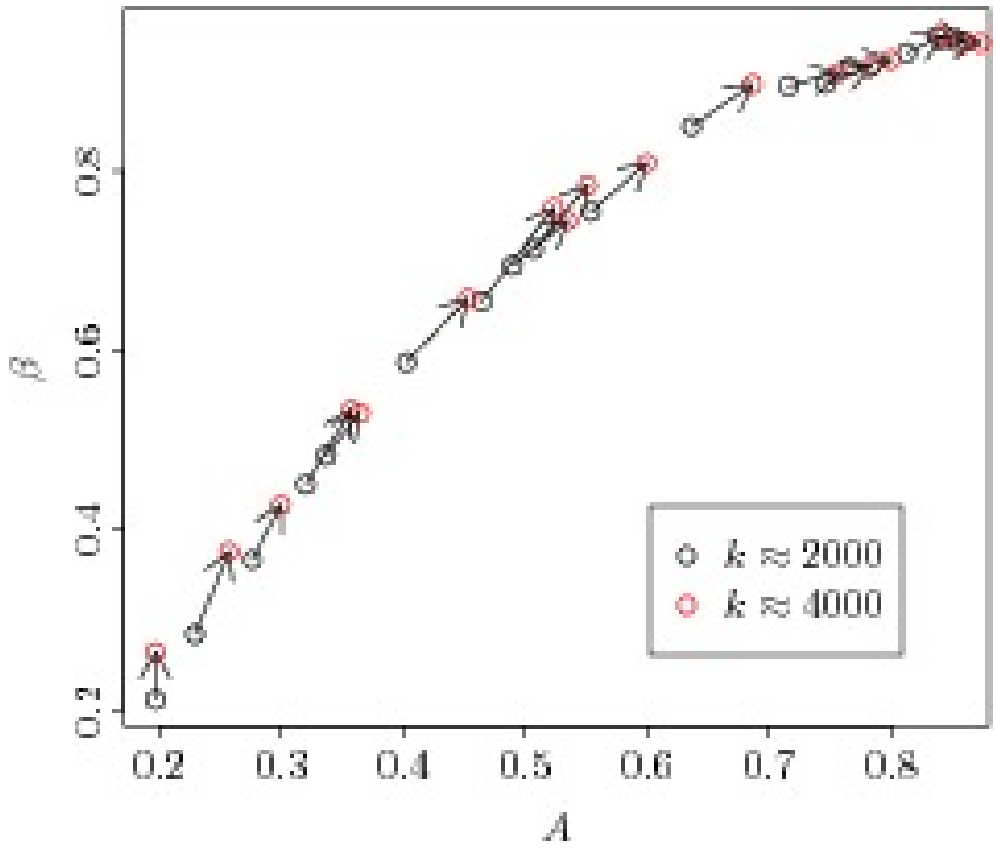

Arrows connect points corresponding to the same λ at two different k.

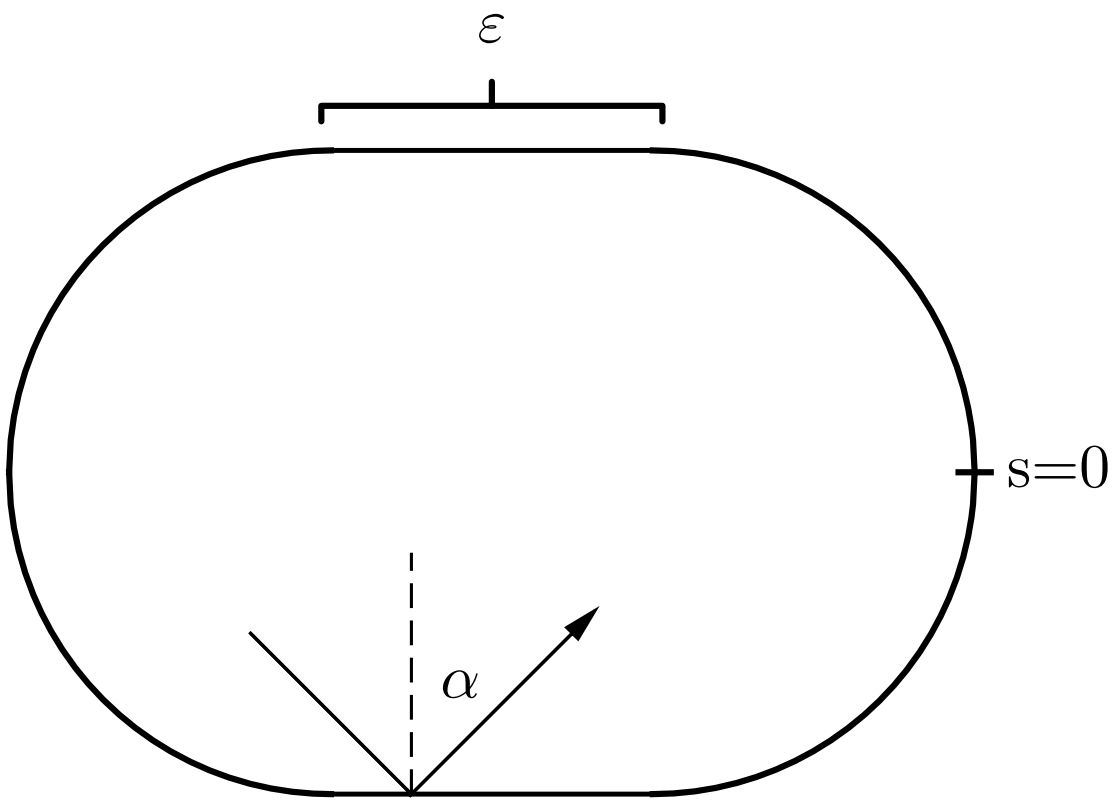

The geometry and notation of the stadium billiard of Bunimovich. ϵ is the family parameter. The larger ϵ the stronger chaos.

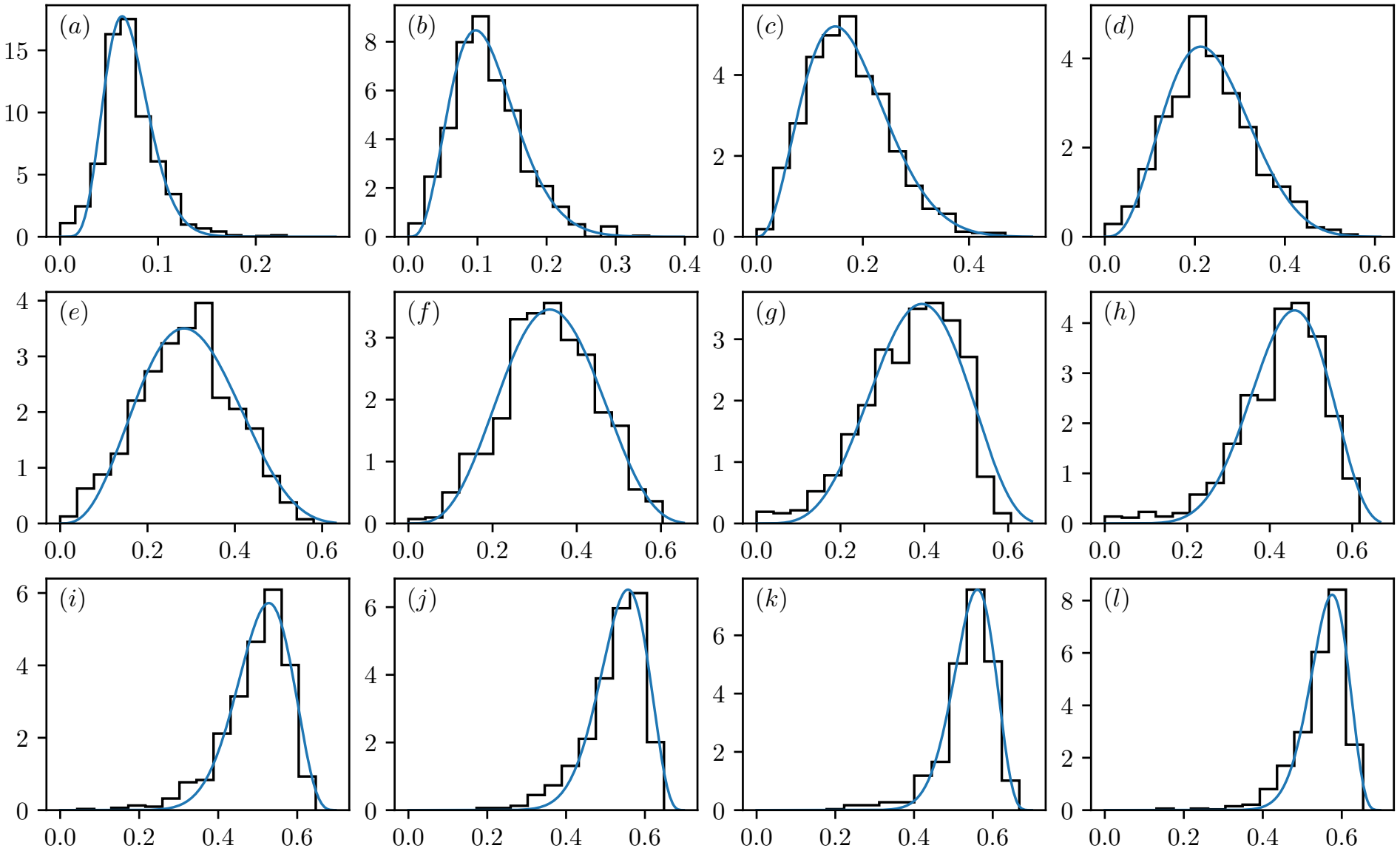

The distributions $P(A)$ of the entropy localization measure A for $k_0 = 3440$ and various ϵ (from (a) to (l)): 0.02, 0.03, 0.04, 0.05, 0.06, 0.07, 0.08, 0.1, 0.14, 0.16, 0.18, 0.2. Blue line: Beta distribution $P(A) = CA^a(A_0 - A)^b$, with $A_0 = 0.7$.

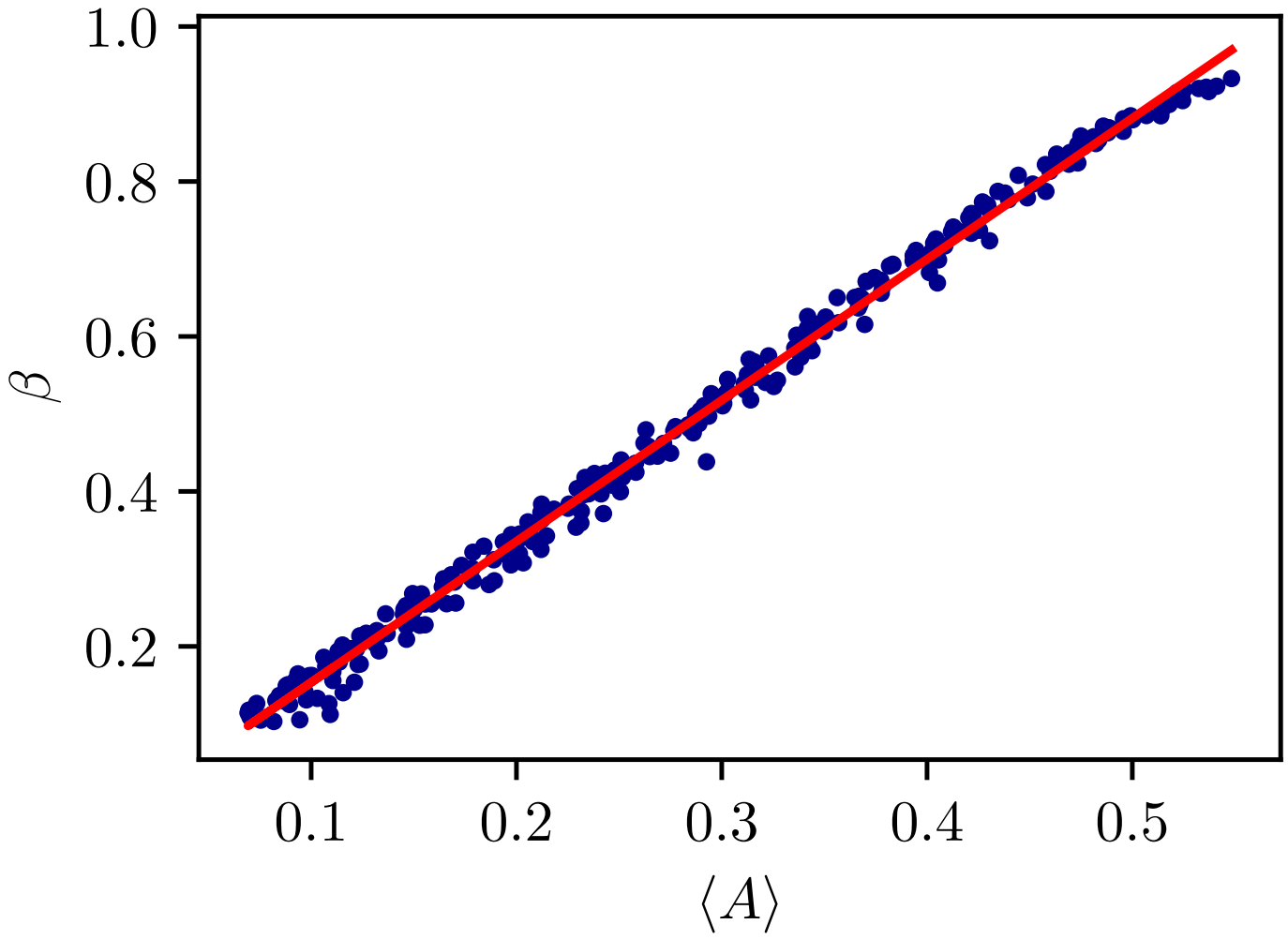

The level repulsion exponent β as a function of the entropy localization measure $\langle A \rangle$ for variety of stadia of different shapes ϵ and energies $E = k^2$, as defined in the text.

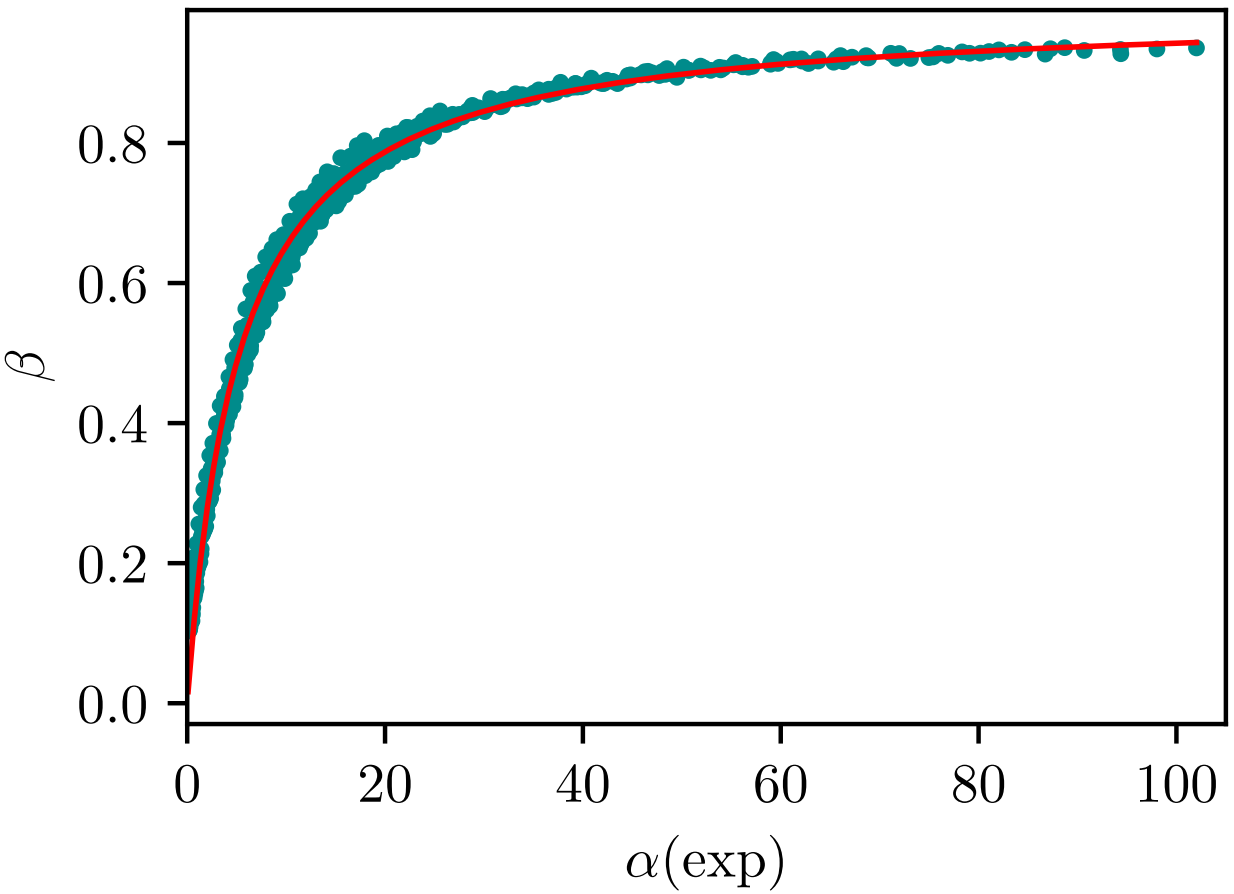

The level repulsion exponent β as a function of

$\alpha =$ Heisenberg time/classical transport time

fitted by the rational function $\beta = \beta_\infty \frac{s\alpha}{1+s\alpha}$, based on the classical transport time from the exponential diffusion law. $\beta_\infty = 0.98$ and $s = 0.20$.

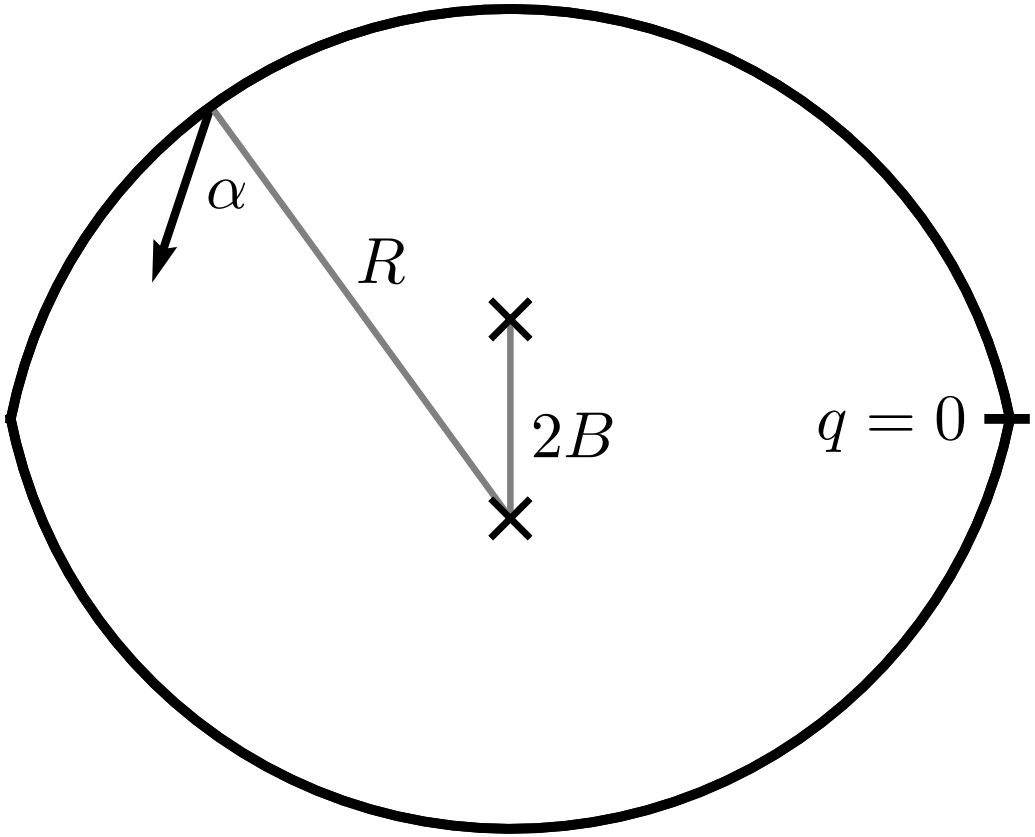

Lemon billiard with the shape parameter B.

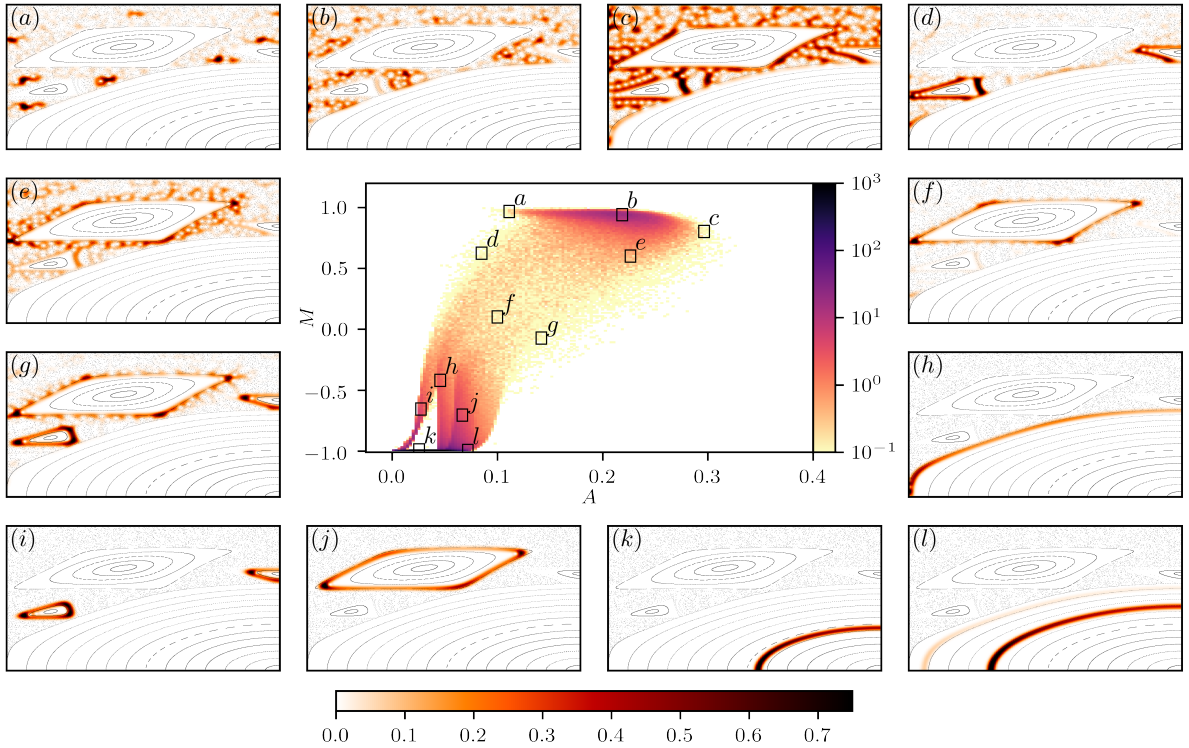

Central: color-plot of the histogram of the joint probability density $P(A, M)$ for approximately 10^6 eigenstates with unfolded energy $e \in [10^4, 10^6]$ of the $B = 0.1953$ lemon billiard. The color scale of the main figure is logarithmic. PH functions of the highest energy eigenstates within small boxes at various positions are shown on the margin. A classical phase portrait is plotted in the background of each state for comparison.The color scale at the bottom encodes the relative amplitude of the PH function.

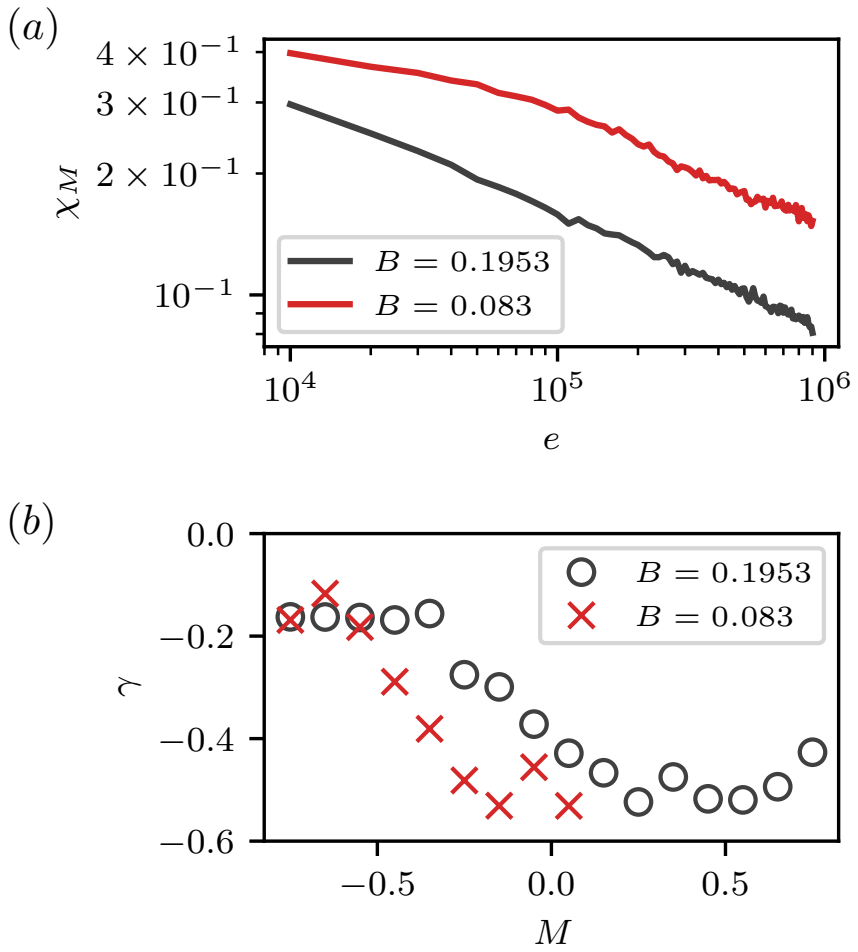

Decay of the relative number of mixed states $|M| \leq 0.8$ with unfolded energy e. (a) The relative number of states in the interval as a function of unfolded energy. Both decay exponents are close to $\gamma = -0.29$. (b) Decay exponents for smaller intervals $[M, M + \delta M]$ with $\delta M = 0.1$.

The Quantum Kicked Top is described by the Hamiltonian

$$H = \alpha J_x + \frac{\gamma}{2j} J_z^2 \sum_{n=-\infty}^{\infty} \delta(t-n),$$

where the dynamical variables of the top are three components of the angular momentum operators of the spin-j system, can also be expressed in terms of $2j$ collective spin-$\frac{1}{2}$ Pauli operators, for example $J_z = \sum_{k=1}^{2j} \sigma_z^{(k)}/2$. The dimension of the Hilbert space is $N = 2j+1$, and the squared angular momentum is conserved, $J^2 = j(j+1)$ with j integer or half-integer. The first term describes a precessional rotation about the x-axis with angular frequency α, the second term denotes a torsional rotation around the z-axis with strength γ (with the period set to unity).

The dynamical evolution of the QKT is governed by the Floquet operator

$$F = \exp(-i\frac{\gamma}{2j} J_z^2) \exp(-i\alpha J_x),$$

and has a well defined classical correspondent in the semiclassical limit.

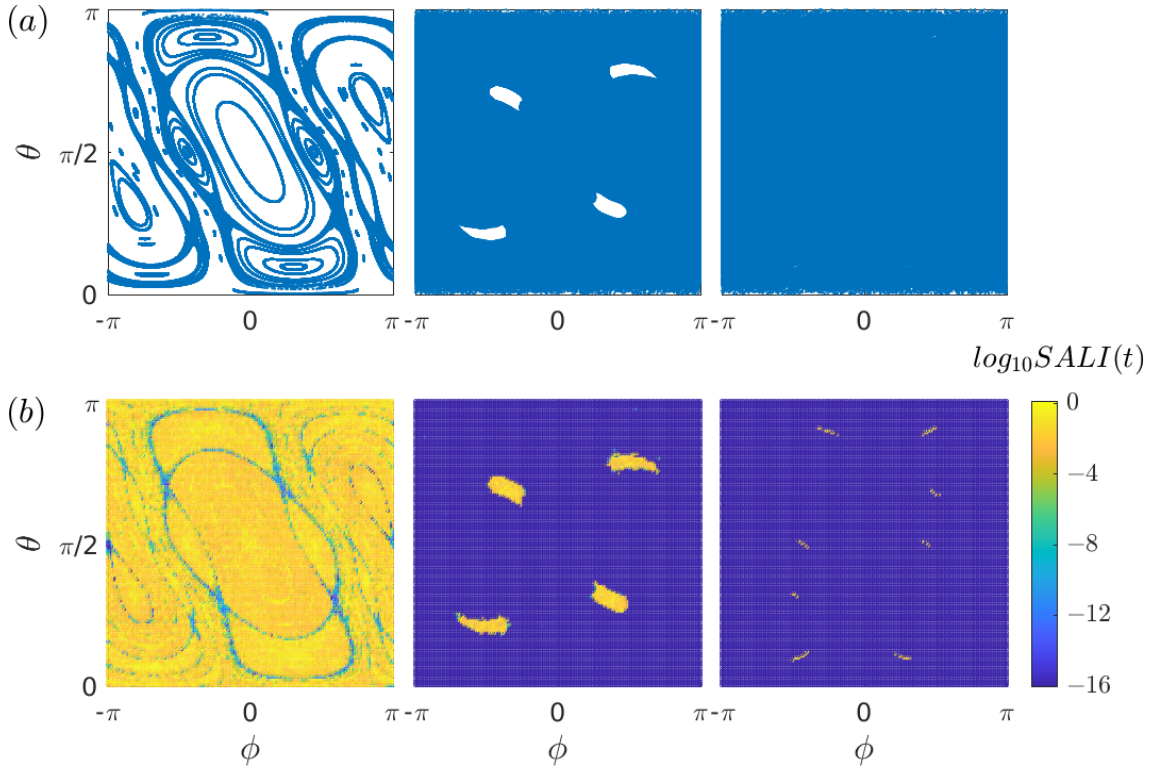

(a) A stroboscopic map of the classical dynamics generated from 20 random initial conditions of 5×10^4 iterations (top panels). (b) The corresponding logarithmic values of SALI (bottom panels) on the parametrized phase space (θ, ϕ) discretized by 200×400 grids of square cells, of same area, after 300 kicks. The initial conditions colored dark blue correspond to chaotic orbits, the yellowish indicates ordered motion, and the intermediate suggests sticky orbits. From left to right, the kicking strength $\gamma = 2, 4, 6$ and $\alpha = 11\pi/19$.

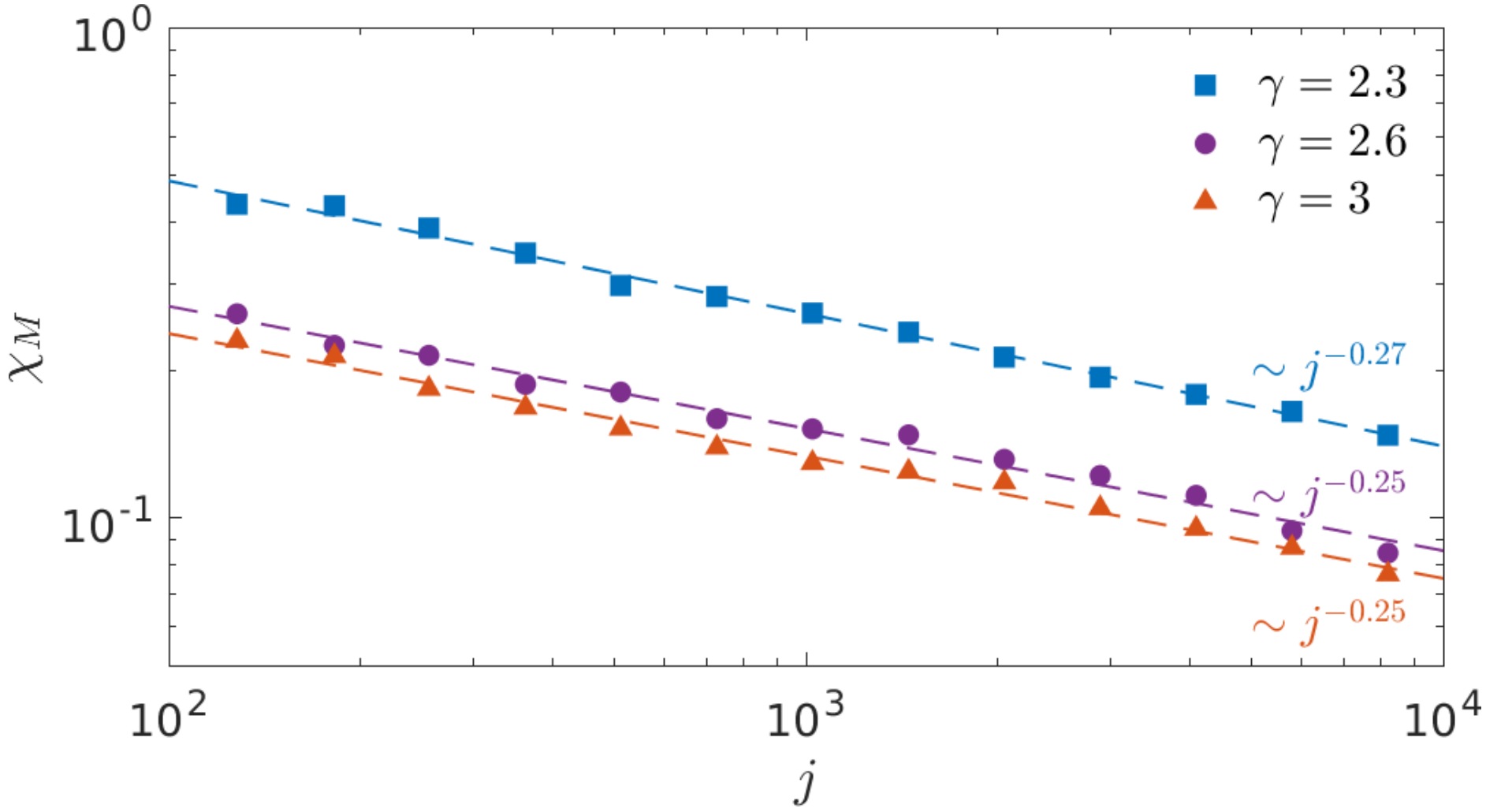

Decay of the fraction of mixed eigenstates χ_M with respect to j, at three kicking strengths $\gamma = 2.3$ (squares), $\gamma = 2.6$ (circles) and $\gamma = 3$ (triangles). The mixed eigenstates criteria here is $M \in [-0.9, 0.5]$. The dashed lines show the power law decay of $\chi_M \sim j^{-\zeta}$.

Discussion and conclusions

• The Principle of Uniform Semiclassical Condensation of Wigner functions of eigenstates leads to the idea that in the sufficiently deep semiclassical limit the spectrum of a mixed type system can be described as a statistically independent superposition of regular and chaotic level sequences.

• As a result of that the $E(k, L)$ probabilities factorize and the level spacings and other statistics can be calculated in a closed form.

• At lower energies we see quantum or dynamical localization.

• The level spacing distribution of localized chaotic eigenstates is excellently described by the Brody distribution with $\beta \in [0, 1]$.

• In the mixed type systems regular and chaotic eigenstates can be separated: the regular obey Poisson, the localized chaotic states obey the Brody.

• The Brody level repulsion exponent β is a function of the mean localization measure $\langle A \rangle$. Both, β and $\langle A \rangle$, are rational functions of α. The transition from strongly localized to fully extended regime is a smooth one.

• The localization measure of chaotic eigenstates exhibits universally beta distribution, if there are no stickiness effects, and else its distribution is system-dependent.

• The distribution of the overlap index M is doubly peaked at the regular end $M = -1$, and at the chaotic end $M = +1$, while the relative fraction of the intermediate values of M, belonging to mixed states, decays as a power law, in accordance with PUSC.

• Such a power law has been found also in the kicked top, Dicke model as an important example of a many-body system and in the FPUT 3-particle system.

Acknowledgements

This work has been supported by the Slovenian Research and Innovation Agency (ARIS), research program P1-0306 and research project J1-4387.